Article

Not peer-reviewed version

Genetic Characteristics of *Acinetobacter baumannii* Isolates Circulating in an Intensive Care Unit of an Infectious Diseases Hospital During the COVID-19 Pandemic

Svetlana S. Smirnova *, Dmitry D. Avdyunin, Marina V. Holmanskikh, Yulia S. Stagilskaya, Nikolai N. Zhuikov, Tarek M. Itani

Posted Date: 5 September 2025

doi: 10.20944/preprints202509.0530.v1

Keywords: *Acinetobacter baumannii*; whole-genome sequencing; antimicrobial resistance; MLST; cgMLST; COVID-19; ICU; hospital environment

Article

Genetic Characteristics of *Acinetobacter baumannii* Isolates Circulating in an Intensive Care Unit of an Infectious Diseases Hospital During the COVID-19 Pandemic

Svetlana S. Smirnova [1,*], Dmitry D. Avdyunin [1], Marina V. Holmanskikh [2], Yulia S. Stagilskaya [1], Nikolai N. Zhuikov [1] and Tarek M. Itani [1]

[1] Federal Scientific Research Institute of Viral Infections «Virome» Rospotrebnadzor, 620030 Yekaterinburg, Russia; Letnyaya Street, 23

[2] The State Autonomous Healthcare Institution of the Sverdlovsk Region "City Infectious Diseases Hospital", 622005 Nizhny Tagil, Russia; Sulfatnaya Street, 4

* Correspondence: smirnova_ss@niivirom.ru; Tel.: +7-(908)-917-59-86

Abstract

During the COVID-19 pandemic, a significant increase in the spread of healthcare-associated infections (HAIs) and antimicrobial resistance (AMR) was observed. *Acinetobacter baumannii*, particularly carbapenem-resistant strains, poses a serious threat in intensive care units (ICUs). This study aimed to genetically characterize *A. baumannii* isolates from the ICU of an infectious diseases hospital repurposed for COVID-19 patient treatment. Whole-genome sequencing (WGS) was performed on 56 *A. baumannii* isolates from patients and environmental surfaces using the Illumina MiSeq platform. Bioinformatic analysis included multi-locus sequence typing (MLST), core-genome MLST (cgMLST), phylogenetic analysis, and in silico detection of antimicrobial resistance genes. Three sequence types (STs) were identified: ST2 (35.7%), ST78 (30.4%), and ST19 (3.5%); while 30.4% of the isolates were non-typeable. Phylogenetic analysis revealed clustering of ST2 with isolates from East Africa, ST78 with European isolates, and ST19 with isolates from Germany and Spain. Resistance genes to eight classes of antimicrobials were detected. All isolates were resistant to aminoglycosides and β-lactams. The *bla*OXA-23 carbapenemase gene was present in all ST2 isolates. cgMLST analysis (cgST-1746) showed significant heterogeneity among ST2 isolates (24–583 allele differences), indicating microevolution within the hospital. A novel synonymous SNP (T2220G) in the *rpoB* gene was identified. Environmental sampling highlighted the role of contaminated personal protective equipment (PPE) in transmission, with 47.0% of ST2 and 64.3% of ST78 isolates found on PPE. The study underscores the high resolution of WGS and cgMLST for epidemiological surveillance and confirms the critical role of infection control measures in preventing the spread of multidrug-resistant *A. baumannii*.

Keywords: *Acinetobacter baumannii*; whole-genome sequencing; antimicrobial resistance; MLST; cgMLST; COVID-19; ICU; hospital environment

1. Introduction

The increasing threat of epidemic-prone infectious diseases is evident from recurrent global outbreaks of emerging viral infections, rising the incidence of healthcare-associated infections (HAIs), and the spread of antimicrobial-resistant (AMR) microorganisms [1]. The prevention of HAIs remains a pressing issue, requiring new approaches in the context of emerging biological threats. In the Russian Federation, the COVID-19 pandemic necessitated the rapid deployment of infectious disease hospitals with segregated "red" and "green" zones, which often led to disruptions in established HAI prevention protocols [2].

 doi:10.20944/preprints202509.0530.v1

These hospitals created dynamic, closed ecosystems where patients underwent numerous invasive procedures, and received antimicrobial treatment, fostering the active circulation of pathogens, their adaptation, and the selection of resistant strains [3]. The spread of HAIs and AMR is a recognized contemporary biological threat, challenging patient safety, healthcare workers, and public health [4,5]. Environmental microorganisms can acquire resistance mechanisms and become clinically significant opportunistic pathogens (OP) upon entering hospital ecosystems [6,7].

Acinetobacter baumannii is a prime example—a ubiquitous environmental bacterium that has evolved into a significant OP in healthcare settings [8,9]. Carbapenem-resistant *A. baumannii* (CRAB) is a leading cause of nosocomial infections in ICUs [10,11]. The COVID-19 pandemic was associated with numerous hospital outbreaks of *A. baumannii*, posing a severe threat to patients [12,13].

Transmission routes in healthcare facilities are diverse, including direct contact, contaminated surfaces, medical devices, and notably, aerosols and personal protective equipment (PPE) [14,15]. *A. baumannii* sequence type 2 (ST2) is a successful, globally distributed clonal lineage associated with outbreaks and multidrug resistance. Classical MLST, based on seven housekeeping genes, lacks the resolution to track the microevolution of *A. baumannii* within a hospital [16].

High-throughput sequencing methods are essential for accurate epidemiological diagnostics, enabling high-resolution typing, relatedness assessment, and detection of resistance and virulence determinants [17–19]. This study aimed to provide a genetic characterization of *A. baumannii* isolates from an infectious diseases' hospital ICU during the COVID-19 pandemic using whole-genome sequencing data.

2. Materials and Methods

2.1. Sampling and Bacterial Isolation

From 2022 to 2023, biological and environmental samples were collected from the infectious diseases hospital for treating COVID-19 patients for the presence of OP. These samples were collected in accordance with a scheme for surface swabs patented by the authors, which was developed for simultaneous assessment of both viral and bacterial contamination [20]. The samples were collected using two swabs pre-moistened in sterile, deionized water simultaneously for three days every four hours at 20 sampling points from environmental surfaces grouped into three blocks: PPE of medical workers (the outer surface of the doctor's/nurse's/orderly's PPE suit, the outer surface of the upper pair of medical gloves: doctor/nurse/orderly), patient care environment (the surface of medical manipulation table, the outer surface of the medical syringe dispenser, handrails and adjustment levers on an ICU bed, the outer surface of the ventilator), general hospital sampling points (The outer surface of the suction unit, dispensers for liquid soap and hand sanitizer, ICU door handles, oxygen pipeline valves, ICU electric light switches, clinical doctor's workspace) (Figure 1).

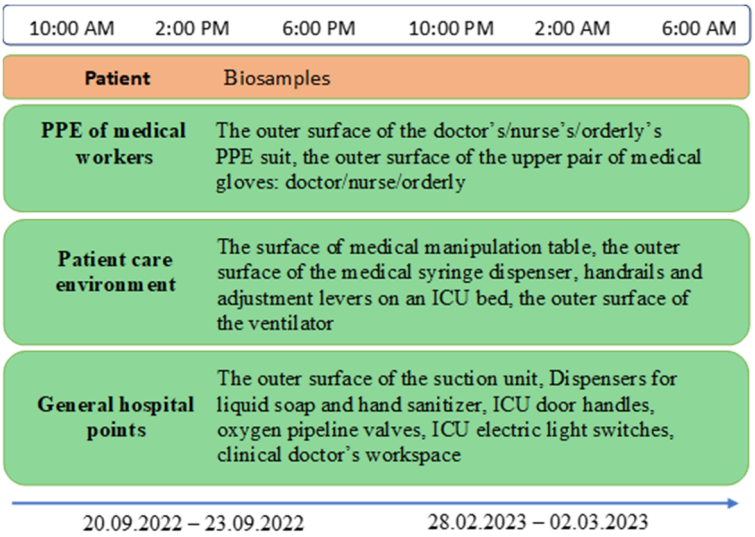

 doi:10.20944/preprints202509.0530.v1

Figure 1. Study design and sampling scheme from patients and the hospital environment.

2.2. DNA Extraction and Whole-Genome Sequencing

DNA extraction was performed using the «RIBO-prep» reagent kit (FBIS CRIE, Moscow) following the manufacturer's protocol. Samples preparation for whole-genome sequencing was conducted in accordance with the Illumina DNA Prep Reference Guide (document #1000000025416 v10) and the LMN DNA LP (M) Tagmentation Kit (Illumina, Singapore). Briefly, DNA libraries were fragmented, and tagged using the transposome included in the kit, with unique indices (DNA/RNA UD Indexes Set A, Tagmentation, Singapore), added to each sample. Samples were normalized, pooled, and subjected to paired-end sequencing on an Illumina MiSeq system with a MiSeq V2 cartridge (300 cycles). Sample preparation and sequencing was done following the manufacturer's protocol.

2.3. Bioinformatic Analysis

Sequencing data quality was assessed using FastQC, evaluating read counts, maximum/minimum read lengths, GC content, and ambiguous nucleotide proportions for forward and reverse reads.

De novo genome assembly was performed via scaffolding using SPAdes 3.15.5 [21] on the Galaxy server, based on paired-end reads. Taxonomic analysis of scaffolds was conducted using Galaxy's FCS GX tool [22] to confirm species identity and remove contaminants. All isolates were confirmed as *A. baumannii*.

Assembled *A. baumannii* sequences were cleaned of residual adapters using NCBI VecScreen: FCS Adaptor [22] and filtered by scaffold length with Trim.seqs 1.39.5 [23].

Typing was performed via multilocus sequence typing (MLST) and core-genome MLST (cgMLST) using the PubMLST database (https://pubmlst.org/).

Multiple sequence alignment and neighbor-joining (NJ) phylogenetic tree construction were performed in Mauve 2.4.0 [24] using the Progressive Mauve algorithm (default parameters: Full Alignment, Sum-of-pairs LCB scoring, HOXD matrix). Scaffolds were aligned to the NCBI reference sequence GCF_009035845.1 (https://www.ncbi.nlm.nih.gov/datasets/genome/GCF_009035845.1/).

In silico detection of antimicrobial resistance (AMR) determinants was conducted using ResFinder 4.6.0 [25] (default thresholds: ≥90% identity, ≥60% coverage). Input data consisted of fastq files (paired-end reads).

Genome annotation was performed via the NCBI Prokaryotic Genome Annotation Pipeline**.** MLST gene alignment and analysis were conducted in MEGA X using the MUSCLE algorithm. The whole genome sequences obtained in this study were submitted to GenBank under accession numbers JBHYBP000000000–JBHYCK000000000, JBITPW000000000–JBITRA000000000.

3. Results

3.1. Isolate Collection and Sequence Types

A total of 56 *A. baumannii* isolates were obtained. MLST analysis successfully typed 39 isolates, revealing ST2 (n=20, 35.7%), ST78 (n=17, 30.4%), and ST19 (n=2, 3.5%). While seventeen isolates (30.4%) were non-typeable (n/d).

ST2 isolates were obtained from patients (15.0%, n=3) and hospital environmental surfaces (85.0%, n=17), with the majority from PPE (47.0%) and patient care environment (41.2%). ST78 isolates were also predominantly isolated from the environmental samples (82.3%, n=14), with most found on PPE (64.3%). Both ST19 isolates were identified in a patient and on PPE.

 doi:10.20944/preprints202509.0530.v1

3.2. Phylogenetic Analysis

Phylogenetic analysis using the PubMLST database (2013–2024) showed that ST2 isolates clustered with samples from East Africa, with sporadic relatedness to Northern and Southern European isolates, suggesting potential introductions to the Russian Federation. ST78 isolates showed relatedness to isolates from Greece, Germany, Finland, Denmark, and Belarus. ST19 isolates were similar to isolates from Germany and Spain (Figure 2).

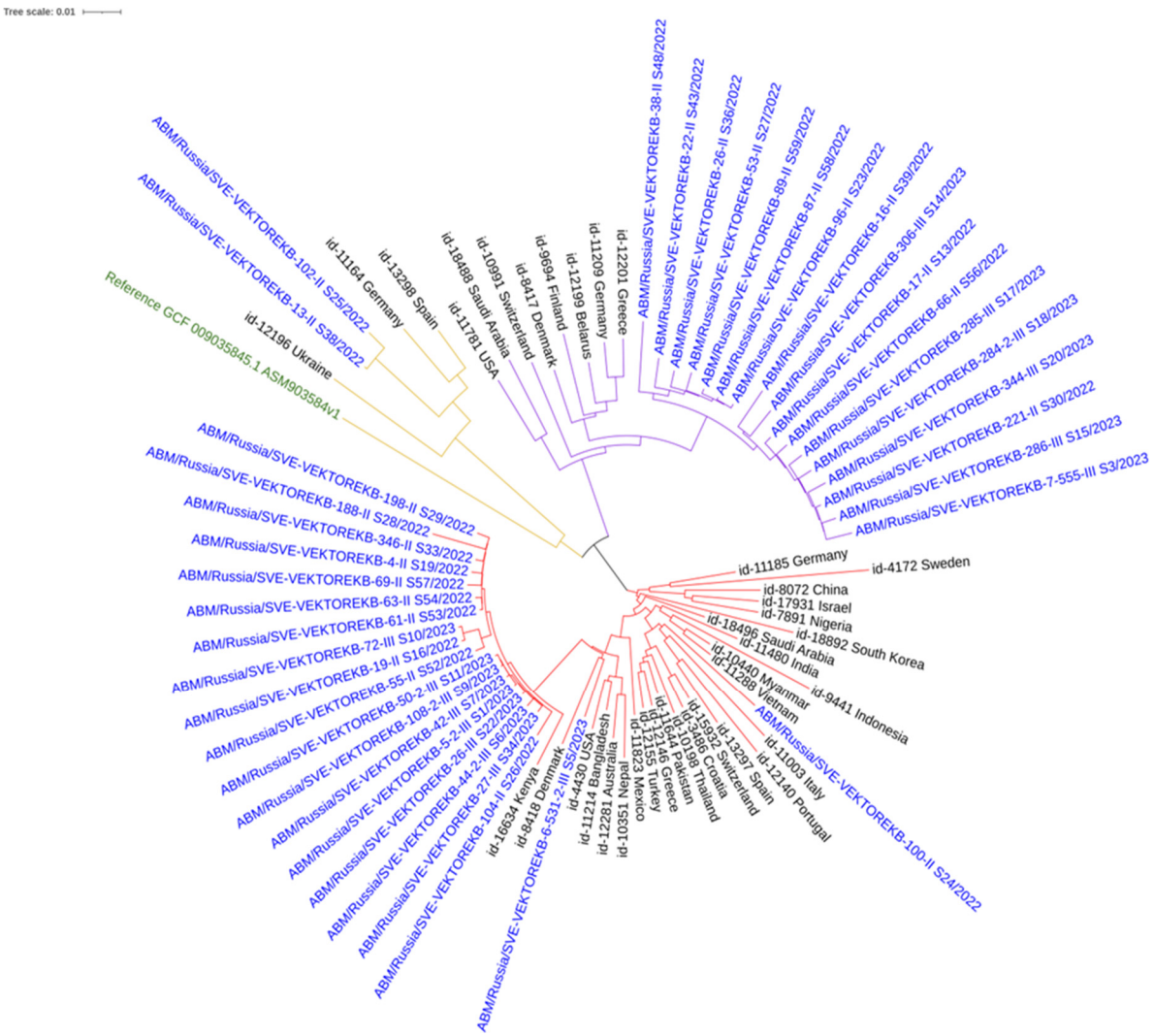

Figure 2. Neighbor-joining phylogenetic tree of *A. baumannii* clinical isolates and reference sequences from the PubMLST database. Colored clades: red (ST2), purple (ST78), yellow (ST19). Blue: study isolates; Black: PubMLST database; Green: GenBank reference.

Within the hospital, clear clustering was observed between patient and environmental isolates. For example, a patient isolate (4-II_S19) clustered with isolates from bed rails, from an orderly's PPE, from and door handles. Another large cluster included isolates from various surfaces (ventilator, PPE of doctors/nurses/orderlies, and manipulation table), underscoring the role of healthcare workers in transmission.

3.3. Antimicrobial Resistance Determinants

Resistance genes to eight antimicrobial classes were identified: aminoglycosides, β-lactams, macrolides, streptogramin B, amphenicols, rifamycins, antifolates, and tetracyclines.
All STs showed 100% prevalence of resistance genes to aminoglycosides and β-lactams.

 doi:10.20944/preprints202509.0530.v1

- **ST2:** Characteristic profile: *armA*, *aph*(*6*)-*Id*, *aph*(*3'*)-*Ia*, *aph*(*3''*)-*Ib*, *bla*OXA-23, *msr(E)*, *mph(E)*. The *bla*OXA-23 carbapenemase was present in 100% of isolates.
- **ST78:** Characteristic profile: *armA*, *bla*OXA-72, *bla*OXA-90, *msr(E)*, *mph(E)*. *bla*OXA-23 was absent.
- **ST19:** Profile included *aph*(*3'*)-*VIa*, *blaOXA-69*, *blaADC-25*, *catA1*, *sul2*, *tet*(*B*).

The n/d group's resistance profile resembled ST2, suggesting possible genetic relatedness or horizontal gene transfer.

When analyzing genetic profiles, isolates were divided into two groups: 1 – patients (*Appendix A.2*); 2 – environmental surfaces (*Appendix A.3*). Isolates from both groups represented all detected ST (Figure. 3). All ST, including n/d group, showed 100% presence of resistance determinants to aminoglycosides and β-lactams, with presumed multidrug resistance (resistance to 4–5 antimicrobial classes) across all groups.

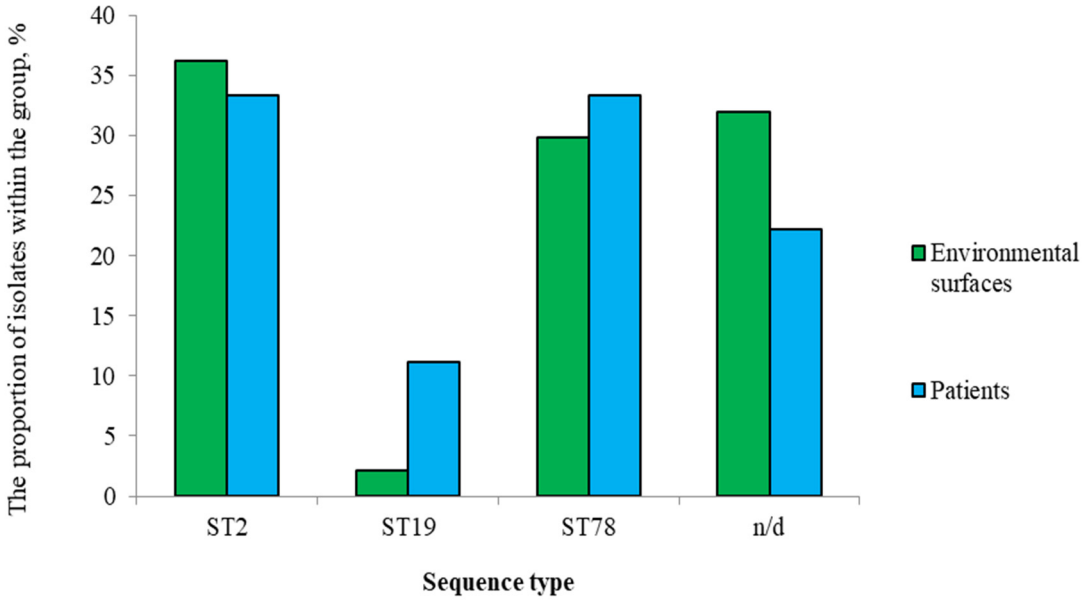

Figure 3. Distribution of *A. baumannii* ST isolated from patients and environmental samples.

3.4. Microevolution and SNP Analysis

Analysis of classical MLST genes for ST2 revealed complete identity with reference sequences. However, cgMLST analysis assigned most isolates to a common cgST-1746 but revealed significant heterogeneity, with allele mismatches ranging from 24 to 583 (Table 1). Isolate 188-II_S28 had the highest number of mismatches (583) and contained a unique synonymous SNP (T2220G) in the *rpoB* gene, not previously reported in databases.

Table 1. Comparative analysis of *A. baumannii* ST2 isolates according to the cgMLST scheme.

Sample ID	Closest cgST	Mismatches, n	Loci matched, %
6-531-2-III_S5	1746	24	98,9
108-2-III_S9	1746	110	94,8
50-2-III_S11	1746	115	95,6
61-II_S53	1746	115	94,6
72-III_S10	1746	117	94,5
42-III_S7	1746	121	94,3

 doi:10.20944/preprints202509.0530.v1

26-III_S22	1746	129	94,0
55-II_S52	1746	138	93,5
19-II_S16	1746	156	92,7
27-III_S34	1746	171	92,0
346-II_S33	1746	186	91,3
63-II_S54	1746	202	90,5
44-2-III_S6	1746	211	90,1
4-II_S19	1746	222	89,6
69-II_S57	1746	228	89,3
198-II_S29	1746	232	89,1
100-II_S24	1746	258	87,9
104-II_S26	1746, 11006	461	78,4
188-II_S28	1746	583	72,7

4. Discussion

One of the most prevalent nosocomial pathogens in modern healthcare settings is *A. baumannii*, which can cause urinary tract infections, bacteremia, meningitis, pneumonia, and catheter-associated infections [26,27]. Immunocompromised systems, particularly those with burn injuries or those admitted to ICU, are at highest risk of infection. The recent COVID-19 pandemic was associated with an increased incidence of ventilator-associated nosocomial secondary infections, for which *A. baumannii* served as a primary etiological agent [28,29].

According to the 2019 Global Antimicrobial Resistance and Use Surveillance System (GLASS) report, 132,000 *A. baumannii* infections directly contributing to patient mortality were resistant to at least one clinically important antibiotic, with 57,700 fatal cases demonstrating carbapenem resistance [30].

The global prevalence of CRAB continues to rise relentlessly, severely limiting treatment options and exacerbating morbidity and mortality rates associated with these infections.

Key mechanisms of carbapenem resistance in *A. baumannii* include enzymatic inactivation, porin modifications, efflux pump upregulation, and β-lactamase production. Among the four known β-lactamase classes (A–D), classes B and D are primarily responsible for carbapenem resistance.

OXA-type carbapenemases (Class D) represent the most prevalent carbapenemases in *A. baumannii*, particularly blaOXA-23-like enzymes. These enzymes are typically plasmid-encoded, facilitating horizontal gene transfer and dissemination within bacterial populations, especially in the hospital environment. The blaOXA-23-like carbapenemase was the first OXA-type carbapenemase identified in CRAB and remains the most globally widespread variant [31]. Consequently, it represents a critical target for molecular surveillance, whose integration into HAIs epidemiological monitoring systems is imperative.

In this study, we showed that ST2 is the predominant lineage in the ICU, with isolates from 3 patients and 17 environmental surfaces (8 from PPE, 7 from patient care areas, and 2 from general hospital sampling points). The prevalence of ST2 reflects the evolutionary success of this clonal lineage (CC2), which accounts for the majority of sequenced genomes globally. The characteristic multidrug resistance profile of ST2 lineage, coupled with limited therapeutic options, ensures its continued prevalence in healthcare facilities [32].

cgMLST analysis revealed a single prevalence cgST-1746 for most isolates. Isolate 104-II_S26 exhibited both cgST-1746 and cgST-11006, while isolate 188-II_S28 (max mismatches=583) contained a unique *rpoB* SNP, potentially indicating accelerated evolutionary adaptation. The mismatch distribution showed no temporal correlation with sampling chronology. The observed cgMLST

 doi:10.20944/preprints202509.0530.v1

heterogeneity despite conserved cgST is characteristic of long-term hospital-adapted populations and reflects the remarkable genomic plasticity of *A. baumannii*.

ST78 represented the second most frequently detected ST, with 3 patient isolates and 14 environmental isolates (9 from PPE, 3 from patient care environment and 2 from hospital sampling points).

ST19 isolates were sporadically detected and did not significantly impact the epidemiological landscape of the COVID-19 ICU.

Beyond antimicrobial resistance mechanisms, *A. baumannii* pathogenicity is mediated by diverse virulence factors. Although virulence determinants remain incompletely characterized, key factors facilitating successful infection include genes encoding outer membrane proteins, biofilm formation machinery, secretion systems, and micronutrient acquisition systems – all warranting further investigation.

Phylogenetic analysis incorporating isolates from the PubMLST international database revealed clustering patterns associated with specific geographic regions, suggesting potential pathogen introductions.

Within the infectious disease hospital, distinct clustering was observed between isolates from patients, medical workers' PPE, and patient environment surfaces. For the two predominant lineages (ST2 and ST78), PPE represented the most contaminated sites (47.0% and 64.3% of isolates, respectively), underscoring the critical importance of strict infection control measures and hygiene practices in healthcare facilities to prevent the spread of antibiotic-resistant bacteria.

In silico analysis identified resistance determinants to eight antimicrobial classes in all *A. baumannii* isolates. Each sequence type exhibited a characteristic resistance profile. All ST2 samples are characterized by a genetic profile of resistance that includes *armA*, *aph*(*6*)-*Id*, *aph*(*3'*)-*Ia*, *aph*(*3''*)-*Ib*, *blaOXA-23*, and *msrI* genes. While, all ST78 samples have a genetic profile of resistance that includes the same resistance genes as ST2, as well as *blaOXA-72* and *blaOXA-90*. Separate resistance genes for various AMR classes have been found in ST19 isolates.

Notably, all ST2 isolates carried the *blaOXA-23* carbapenemase, confirming their CRAB status, while this determinant was absent in ST78 and ST19 lineages. The results are very similar to results published during the same COVID-19 period in Croatia, where *A. baumannii* isolates carrying *blaOXA-23* carbapenemase were identified in ICU patients and air conditioners [33]. This finding is consistent with reports from another Croatian hospital, where CRAB was isolated from hospital surfaces [34], highlighting the role of the contaminated hospital environment in the persistence and spread of these pathogens. Similar results of an *A. baumannii* producing *blaOXA-23* carbapenemase outbreak in Basel, Switzerland were reported in an ICU [35].

One study reported an increased incidence of ventilator-associated pneumonia caused by *A. baumannii* during the pandemic in Mexico. An increase in resistance to aminoglycosides, carbapenems, folate inhibitors and other antibiotics was also observed [36]. Furthermore, the detection of genetic determinants of resistance to these antibiotic classes in our samples is consistent with the observed phenotype of multidrug resistance in *A. baumannii* strains described during the pandemic period.

WGS and cgMLST emerged as the most informative bioinformatics tools, offering superior resolution for HAIs epidemiological surveillance compared to classical MLST approaches.

This study was also only limited to samples collected from one center and from a single ICU. However, the obtained results still emphasize the significance of high-throughput sequencing techniques in studying the biological features of current pathogens. By determining the degree of similarity among isolated strains, identifying their resistance and virulence determinants, and investigating the epidemiological connections between pathogens, we can more accurately identify the key factors contributing to nosocomial infections. These findings will be valuable for developing more efficient strategies to prevent and control infections caused by *A. baumannii* in hospital settings.

 doi:10.20944/preprints202509.0530.v1

5. Conclusions

In conclusion, the ICU environment during the COVID-19 pandemic was dominated by MDR *A. baumannii* ST2, harboring the *armA* 16S rRNA methylstransferase and the *bla*OXA-23 carbapenemase. The study demonstrates the critical role of contaminated environmental surfaces, especially PPE, in the transmission chain. The high resolution of WGS and cgMLST is essential for effective epidemiological surveillance and outbreak investigation. These findings emphasize the need for reinforced infection prevention and control measures in healthcare settings managing vulnerable patient populations.

Author Contributions: Conceptualization, S.S.S. and N.N.Z.; methodology, S.S.S., D.D.A. and T.M.I.; software, D.D.A.; validation, Y.S.S. and N.N.Z.; formal analysis, D.D.A.; investigation, S.S.S., Y.S.S., N.N.Z. and T.M.I.; resources, M.V.H.; data curation, D.D.A.; writing—original draft preparation, D.D.A. and S.S.S.; writing—review and editing, all authors; visualization, D.D.A.; supervision, S.S.S.; project administration, S.S.S.; funding acquisition, S.S.S. All authors have read and agreed to the published version of the manuscript.

Funding: This research was funded by the Russian scientific project "Study of the epidemic process and prevention of viral healthcare-associated infections", Reg. No. 121040500099-5.

Institutional Review Board Statement: The study was conducted in accordance with the Declaration of Helsinki and approved by the Local Ethics Committee of the State Scientific Center of Virology and Biotechnology "Vector" (protocol code № 3, date of approval 24 June 2022).

Informed Consent Statement: Patient consent was waived due to the retrospective nature of the study and the use of anonymized bacterial isolates obtained as part of routine clinical microbiological surveillance.

Data Availability Statement: The raw sequencing data generated in this study have been deposited in the NCBI SRA database under BioProject accession number PRJNA1165946.

Acknowledgments: The authors thank the staff of the Nizhny Tagil City Infectious Diseases Hospital for their assistance in sample collection.

Conflicts of Interest: The authors declare no conflicts of interest.

Abbreviations

AMR	Antimicrobial resistance
CRAB	Carbapenem-resistant *A. baumannii*
cgMLST	Core-genome MLST
ICUs	Intensive care units
HAIs	Healthcare-associated infections
OP	Opportunistic pathogen
MLST	Multi-locus sequence typing
PPE	Personal protective equipment
ST	Sequence type
WGS	Whole-genome sequencing
PCE	Patient care environment
GHP	General hospital point
AMI	Aminoglicoside
BL	Beta-lactam
MKL	Macrolide
SGB	Streptogramin b
AP	Amphenicol
RF	Rifamycin
AF	Antifolates

 doi:10.20944/preprints202509.0530.v1

TET Tetracycline

Appendix A

Appendix A.1

Sample ID	Selection group	Selection point
5-2-III_S1	PPE	The outer surface of the **upper pair of medical gloves (orderly)**
6-2-III_S35	PPE	The outer surface of the orderly's PPE suit
7-II_S40	PCE	The surface of **medical manipulation table**
13-2-II_S41	PCE	The outer surface of the medical syringe dispenser
21-II_S42	PPE	The outer surface of the **upper pair of medical gloves (doctor)**
22-II_S43	PPE	The outer surface of the **upper pair of medical gloves (nurse)**
25-II_S45	PPE	The outer surface of the orderly's PPE suit
26-II_S36	PPE	The outer surface of the doctor's PPE suit
26-III_S22	PPE	The outer surface of the orderly's PPE suit
27-III_S34	PCE	The surface of **medical manipulation table**
28-II_S46	PCE	Handrails and adjustment levers on an ICU bed
33-II_S47	PCE	The outer surface of the medical syringe dispenser
38-II_S48	GHP	ICU door handles
42-III_S7	PPE	The outer surface of the doctor's PPE suit
44-2-III_S6	PPE	The outer surface of the nurse's PPE suit
48-2-III_S4	PCE	Handrails and adjustment levers on an ICU bed
48-II_S49	PCE	The surface of **medical manipulation table**
49-II_S50	PCE	Handrails and adjustment levers on an ICU bed
50-2-III_S11	PCE	**The outer surface of the ventilator**
51-II_S51	PCE	**The outer surface of the ventilator**
53-II_S27	PCE	Handrails and adjustment levers on an ICU bed
55-II_S52	PCE	**The outer surface of the ventilator**
61-II_S53	PPE	The outer surface of the **upper pair of medical gloves (orderly)**
63-II_S54	PPE	The outer surface of the **upper pair of medical gloves (nurse)**
64-II_S55	PPE	The outer surface of the nurse's PPE suit
66-II_S56	PPE	The outer surface of the doctor's PPE suit
69-II_S57	PCE	Handrails and adjustment levers on an ICU bed
72-III_S10	PCE	Handrails and adjustment levers on an ICU bed
87-II_S58	PCE	The surface of **medical manipulation table**
89-II_S59	PCE	Handrails and adjustment levers on an ICU bed
96-II_S23	GHP	The outer surface of the suction unit
100-II_S24	GHP	Dispensers for liquid soap and hand sanitizer
102-II_S25	PPE	The outer surface of the nurse's PPE suit
104-II_S26	PPE	The outer surface of the orderly's PPE suit
108-2-III_S9	PCE	Handrails and adjustment levers on an ICU bed
188-II_S28	PCE	Handrails and adjustment levers on an ICU bed
198-II_S29	GHP	ICU door handles
221-II_S30	PPE	The outer surface of the **upper pair of medical gloves (doctor)**
284-2-III_S18	PPE	The outer surface of the nurse's PPE suit
285-III_S17	PPE	The outer surface of the **upper pair of medical gloves (orderly)**
286-III_S15	PPE	The outer surface of the orderly's PPE suit
306-III_S14	PPE	The outer surface of the orderly's PPE suit
307-1-II_S32	PCE	The surface of **medical manipulation table**
331-II_S12	PCE	The surface of **medical manipulation table**
344-III_S20	PPE	The outer surface of the nurse's PPE suit
346-II_S33	PPE	The outer surface of the orderly's PPE suit
224-2_S15	PPE	The outer surface of the doctor's PPE suit

Notes: PPE – personal protective equipment, PCE – patient care environment, GHP – general hospital point.

Appendix A.2

Genetic determinants profiles of resistance of patient's *A. baumannii* isolates

Sample ID	ML ST	AMI								BL									MKL	SGB	AP				RF	AF		TET
		armA	*aph(6)-Id*	*aph(3'')-Ia*	*aph(3')-VIa*	*aph(3'')-Ib*	*aph(3')-VIb*	*aadA1*	*aac(6')-Ib3*	*blaOXA-23*	*blaADC-25*	*blaPER-7*	*blaOXA-66*	*blaCTX-M-*	*blaOXA-72*	*blaOXA-90*	*blaTEM-1D*	*blaCARB-14*	*msr(E)*	*mph(E)*	*catB8*	*cmlA1*	*floR*	*catA1*	*ARR-2*	*sul1*	*sul2*	*tet(B)*
2-II_S37	n/d	1	1	1	0	1	0	1	0	1	1	1	0	0	0	0	0	0	1	1	1	1	0	0	1	1	1	0
4-II_S19	ST2	1	1	1	0	1	0	1	1	1	1	1	1	0	0	0	0	0	1	1	1	0	0	0	1	0	0	0
6-531-2-III_S5	ST2	1	1	1	0	1	0	1	1	1	1	0	1	0	0	0	0	0	1	1	1	0	0	0	0	0	1	0
7-555-III_S3	ST78	1	0	0	0	0	0	0	0	0	1	0	0	1	1	1	0	0	1	1	0	0	0	1	0	0	0	0
13-II_S38	ST19	0	0	0	1	0	0	0	0	0	1	0	0	0	0	0	0	0	0	0	0	0	0	1	0	0	1	1
14-II_S21	n/d	1	1	1	0	1	1	0	0	1	0	0	0	0	0	0	1	1	1	1	0	0	1	0	0	0	0	1
16-II_S39	ST78	1	0	0	0	0	0	0	0	0	1	0	0	1	1	1	0	0	1	1	0	0	0	1	0	0	0	0
17-II_S13	ST78	1	0	0	0	0	0	0	0	0	1	0	0	0	1	1	0	0	1	1	0	0	0	0	0	0	0	0
19-II_S16	ST2	1	1	1	0	1	0	1	1	1	1	0	1	0	0	0	0	0	1	1	1	1	0	0	1	1	1	0

Notes: AMI – aminoglicoside; BL – beta-lactam; MKL – macrolide; SGB – streptogramin b; AP – amphenicol; RF – rifamycin; AF – antifolates; TET – tetracycline; 1 – is available; 0 – absent.

Appendix A.3

Genetic determinants profiles of resistance of environmental objects' *A. baumannii* isolates

Sample ID	ML ST	AMI								BL									MKL	SGB	AP				RF	AF		TET
		armA	*aph(6)-Id*	*aph(3")-Ia*	*aph(3')-*	*aph(3")-*	*aph(3')-*	*aadA1*	*aac(6')-Ib3*	*blaOXA-*	*blaADC-*	*blaPER-7*	*blaOXA-*	*blaCTX-*	*blaOXA-*	*blaOXA-*	*blaTEM-*	*blaCARB-*	*msr(E)*	*mph(E)*	*catB8*	*cmlA1*	*floR*	*catA1*	*ARR-2*	*sul1*	*sul2*	*tet(B)*
5-2-III_S1	ST2	1	1	1	0	1	0	1	1	1	1	0	1	0	0	0	0	0	1	1	1	1	0	0	1	1	1	0
6-2-III_S35	n/d	1	1	1	0	1	0	1	1	1	1	0	0	0	0	0	0	0	1	1	1	1	0	0	1	1	1	0
7-II_S40	n/d	1	1	1	0	1	0	1	1	1	1	1	1	0	0	0	0	0	1	1	1	1	0	0	1	1	1	0
13-2-II_S41	n/d	1	0	0	0	0	0	0	0	0	0	0	0	1	1	1	0	0	1	1	0	0	0	1	0	0	0	0
21-II_S42	n/d	0	0	0	1	0	0	0	0	0	1	0	1	0	0	0	0	0	0	0	0	0	0	1	0	0	1	1
22-II_S43	ST78	1	0	0	0	0	0	0	0	0	1	0	0	1	1	1	0	0	1	1	0	0	0	1	0	0	0	0
25-II_S45	n/d	1	0	0	0	0	0	0	0	0	0	0	0	1	1	1	0	0	1	1	0	0	0	1	0	0	0	0
26-II_S36	ST78	1	0	0	0	0	0	0	0	0	1	0	0	1	1	1	0	0	1	1	0	0	0	1	0	0	0	0
26-III_S22	ST2	1	1	1	0	1	0	1	1	1	1	0	1	0	0	0	0	0	1	1	1	1	0	0	1	1	1	0
27-III_S34	ST2	1	1	1	0	1	0	1	1	1	1	0	1	0	0	0	0	0	1	1	1	1	0	0	1	1	1	0
28-II_S46	n/d	1	1	1	0	1	0	1	1	1	1	1	0	0	0	0	0	0	1	1	1	1	0	0	1	1	1	0
33-II_S47	n/d	1	1	1	0	1	0	1	1	1	0	1	0	0	0	0	0	0	1	1	1	1	0	0	1	1	1	0

38-II_S48	ST78	1	0	0	0	0	0	0	0	0	1	0	0	1	1	1	0	0	1	1	0	0	0	1	0	0	0	0
42-III_S7	ST2	1	1	1	0	1	0	1	1	1	1	0	1	0	0	0	0	0	1	1	1	1	0	0	1	1	1	0
44-2-III_S6	ST2	1	1	1	0	1	0	1	1	1	1	0	0	0	0	0	0	0	1	1	1	1	0	0	1	1	1	0
48-2-III_S4	n/d	1	1	1	0	1	0	1	1	1	0	0	0	0	0	0	0	0	1	1	1	1	0	0	1	1	1	0
48-II_S49	n/d	1	1	1	0	1	0	0	1	1	1	1	1	0	0	0	0	0	1	1	1	1	0	0	1	0	1	0
49-II_S50	n/d	1	1	1	0	1	0	1	1	1	0	1	0	0	0	0	0	0	1	1	1	1	0	0	1	1	1	0
50-2-III_S11	ST2	1	1	1	0	1	0	1	1	1	1	0	1	0	0	0	0	0	1	1	1	1	0	0	1	0	0	0
51-II_S51	n/d	1	1	1	0	1	0	1	1	1	0	1	0	0	0	0	0	0	1	1	1	1	0	0	1	0	0	0
53-II_S27	ST78	1	0	0	0	0	0	0	0	0	1	0	0	1	1	1	0	0	1	1	0	0	0	1	0	0	0	0
55-II_S52	ST2	1	1	1	0	1	0	1	1	1	1	1	1	0	0	0	0	0	1	1	1	1	0	0	1	1	1	0
61-II_S53	ST2	1	1	1	0	1	0	1	1	1	1	1	1	0	0	0	0	0	1	1	1	1	0	0	1	1	1	0
63-II_S54	ST2	1	1	1	0	1	0	1	1	1	1	1	1	0	0	0	0	0	1	1	1	1	0	0	1	1	1	0
64-II_S55	n/d	1	1	1	0	1	0	1	1	1	0	1	0	0	0	0	0	0	1	1	1	1	0	0	1	1	1	0
66-II_S56	ST78	1	0	0	0	0	0	0	0	0	1	0	0	0	1	1	0	0	1	1	0	0	0	0	0	0	0	0
69-II_S57	ST2	1	1	1	0	1	0	1	1	1	1	1	1	0	0	0	0	0	1	1	1	1	0	0	1	1	1	0
72-III_S10	ST2	1	1	1	0	1	0	1	1	1	1	0	1	0	0	0	0	0	1	1	1	1	0	0	1	1	1	0
87-II_S58	ST78	1	0	0	0	0	0	0	0	0	1	0	0	1	1	1	0	0	1	1	0	0	0	1	0	0	0	0
89-II_S59	ST78	1	0	0	0	0	0	0	0	0	1	0	0	1	1	1	0	0	1	1	0	0	0	1	0	0	0	0

96-II_S23	ST78	1	0	0	0	0	0	0	0	0	1	0	0	1	1	1	0	0	1	1	0	0	0	1	0	0	0	0
100-II_S24	ST2	1	1	1	0	1	1	0	0	1	1	0	1	0	0	0	1	1	1	1	0	0	1	0	0	0	1	1
102-II_S25	ST19	0	0	0	1	0	0	0	0	0	1	0	1	0	0	0	0	0	0	0	0	0	0	1	0	0	1	1
104-II_S26	ST2	1	1	1	0	1	0	1	1	1	0	0	0	0	0	0	0	0	0	0	1	1	1	1	0	0	1	1	1	0
108-2-III_S9	ST2	1	1	1	0	1	0	1	1	1	1	0	1	0	0	0	0	0	1	1	1	1	0	0	1	1	1	0
188-II_S28	ST2	1	1	1	0	1	0	1	1	1	0	1	0	0	0	0	0	0	1	1	1	1	0	0	1	1	1	0
198-II_S29	ST2	1	1	1	0	1	0	1	1	1	1	1	1	0	0	0	0	0	1	1	1	1	0	0	1	1	1	0
221-II_S30	ST78	1	0	0	0	0	0	0	0	0	1	0	0	1	1	1	0	0	1	1	0	0	0	1	0	0	0	0
284-2-III_S18	ST78	1	0	0	0	0	0	0	0	0	0	0	0	1	1	1	0	0	1	1	0	0	0	1	0	0	0	0
285-III_S17	ST78	1	0	0	0	0	0	0	0	0	1	0	0	1	1	1	0	0	1	1	0	0	0	1	0	0	0	0
286-III_S15	ST78	1	0	0	0	0	0	0	0	0	1	0	0	1	1	1	0	0	1	1	0	0	0	1	0	0	0	0
306-III_S14	ST78	1	0	0	0	0	0	0	0	0	1	0	0	1	1	1	0	0	1	1	0	0	0	1	0	0	0	0
307-1-II_S32	n/d	1	1	1	0	1	1	1	0	1	1	1	0	0	0	0	0	0	1	1	1	1	0	0	1	1	1	0

331-II_S12	n/d	1	0	0	0	0	0	0	0	0	1	0	0	1	1	1	0	0	1	1	0	0	0	1	0	0	0	0
344-III_S20	ST78	1	0	0	0	0	0	0	0	0	1	0	0	1	1	1	0	0	1	1	0	0	0	1	0	0	0	0
346-II_S33	ST2	1	1	1	0	1	0	1	1	1	1	1	1	0	0	0	0	0	1	1	1	1	0	0	1	1	1	0
224-2_S15	n/d	1	0	0	0	0	0	0	0	0	0	0	0	1	1	0	0	0	1	1	0	0	0	1	0	0	0	0

Notes: AMI – aminoglicoside; BL – beta-lactam; MKL – macrolide; SGB – streptogramin b; AP – amphenicol; RF – rifamycin; AF – antifolates; TET – tetracycline; 1 – is available; 0 – absent.

 doi:10.20944/preprints202509.0530.v1

References

1. Ivanov, F.V.; Gumilyevsky, B.Y. Microbiological Monitoring of Healthcare-Associated Infections. *Mezhdunarodnyj Nauchno-Issledovatel'skij Zhurnal* **2023**, *138*, 210. https://doi.org/10.23670/IRJ.2023.138.210 (In Russian)
2. Kutyrev, V.V.; Popova, A.Y.; Smolensky, V.Y.; et al. Epidemiological Features of the New Coronavirus Infection (COVID-19). Message 2. *Probl Osobo Opasnykh Infektsii* **2020**, *2*, 6–12. https://doi.org/10.21055/0370-1069-2020-2-6-12 (In Russian)
3. Brusina, E.B.; Zueva, L.P.; Kovalishena, O.V.; et al. Infections Related To Medical Care: A Modern Prevention Doctrine. *Epidemiol Vakcinoprofilaktika* **2018**, *17*, 4–10. https://doi.org/10.31631/2073-3046-2018-17-4-10 (In Russian)
4. O'Toole, R.F. The Interface Between COVID-19 and Bacterial Healthcare-Associated Infections. *Clin Microbiol Infect* **2021**, *27*, 1772–1776. https://doi.org/10.1016/j.cmi.2021.06.001
5. Mustapha, M.M.; Srinivasa, V.R.; Griffith, M.P.; et al. Genomic Diversity of Hospital-Acquired Infections Revealed through Prospective Whole-Genome Sequencing-Based Surveillance. *mSystems* **2022**, *7*, e0138421. https://doi.org/10.1128/msystems.01384-21
6. Larsson, D.G.J.; Flach, C.F. Antibiotic Resistance in the Environment. *Nat Rev Microbiol* **2022**, *20*, 257–269. https://doi.org/10.1038/s41579-021-00649-x
7. Weimann, A.; Dinan, A.M.; Ruis, C.; et al. Evolution and Host-Specific Adaptation of *Pseudomonas aeruginosa*. *Science* **2024**, *385*, eadi0908. https://doi.org/10.1126/science.adi0908
8. Wen, H.; Wang, K.; Liu, Y.; et al. Population Dynamics of an *Acinetobacter baumannii* Clonal Complex during Colonization of Patients. *J Clin Microbiol* **2014**, *52*, 3200–3208. https://doi.org/10.1128/JCM.00921-14
9. Roca, I.; Espinal, P.; Vila-Farrés, X.; Vila, J. The *Acinetobacter baumannii* Oxymoron: Commensal Hospital Dweller Turned Pan-Drug-Resistant Menace. *Front Microbiol* **2012**, *3*, 148. https://doi.org/10.3389/fmicb.2012.00148
10. Antunes, L.C.; Visca, P.; Towner, K.J. *Acinetobacter baumannii*: Evolution of a Global Pathogen. *Pathog Dis* **2014**, *71*, 292–301. https://doi.org/10.1111/2049-632X.12125
11. Abdul-Mutakabbir, J.C.; Griffith, N.C.; Shields, R.K.; et al. Contemporary Perspective on the Treatment of *Acinetobacter baumannii* Infections: Insights from the Society of Infectious Diseases Pharmacists. *Infect Dis Ther* **2021**, *10*, 2177–2202. https://doi.org/10.1007/s40121-021-00541-4
12. Boral, J.; Genç, Z.; Pınarlık, F.; et al. The Association Between *Acinetobacter baumannii* Infections and the COVID-19 Pandemic in an Intensive Care Unit. *Sci Rep* **2022**, *12*, 20808. https://doi.org/10.1038/s41598-022-25493-8
13. Noskov, A.K.; Popova, A.Y.; Vodopyanov, A.S.; et al. Molecular Genetic Analysis of Bacterial Pneumonia Pathogens Associated with COVID-19 in Rostov-on-Don Hospitals. *Zdorov'e Naselenija i Sreda Obitanija* **2021**, *29*, 64–71. https://doi.org/10.35627/2219-5238/2021-29-12-64-71 (In Russian)
14. Fröhlich-Nowoisky, J.; et al. Bioaerosols in the Earth System: Climate, Health, and Ecosystem Interactions. *Atmospheric Res* **2016**, *182*, 346–376. https://doi.org/10.1016/j.atmosres.2016.07.018
15. Khan, B.A.; Roy, S.; Tahsin, N.; et al. Antibiotic Resistance of Bioaerosols in Particulate Matter from Indoor Environments of the Hospitals in Dhaka Bangladesh. *Sci Rep* **2024**, *14*, 29884. https://doi.org/10.1038/s41598-024-81376-0
16. Bartual, S.G.; Seifert, H.; Hippler, C.; et al. Development of a Multilocus Sequence Typing Scheme for Characterization of Clinical Isolates of *Acinetobacter baumannii*. *J Clin Microbiol* **2005**, *43*, 4382–4390. https://doi.org/10.1128/JCM.43.9.4382-4390.2005
17. Park, S.; Ryoo, N. Comparative Analysis of IR-Biotyper, MLST, cgMLST, and WGS for Clustering of Vancomycin-Resistant *Enterococcus faecium* in a Neonatal Intensive Care Unit. *Microbiol Spectr* **2024**, *12*, e0411923. https://doi.org/10.1128/spectrum.04119-23
18. Heneghan, C.J.; Spencer, E.A.; Brassey, J.; et al. SARS-CoV-2 and the Role of Orofecal Transmission: A Systematic Review. *F1000Research* **2021**, *10*, 231. https://doi.org/10.12688/f1000research.51592.2
19. Poslova, L.Y.; Sergeeva, A.V.; Kovalishena, O.V. Assessment of Contamination of the Hospital Environment with Intestinal Viruses in the Framework of Epidemiological Surveillance of Acute Intestinal Infections of Viral Etiology. *Epidemiologiya* **2018**, *4*, 42–46. (In Russian)

 doi:10.20944/preprints202509.0530.v1

20. Smirnova, S.S.; Zhuikov, N.N.; Egorov, I.A.; et al. Industrial Design Patent No. 132971 Russian Federation. Sampling Scheme of Flushes from Environmental Objects for Simultaneous Assessment of Viral and Bacterial Contamination: No. 2022501675. 2022. (In Russian)
21. Bankevich, A.; Nurk, S.; Antipov, D.; et al. SPAdes: A New Genome Assembly Algorithm and Its Applications to Single-Cell Sequencing. *J Comput Biol* **2012**, *19*, 455–477. https://doi.org/10.1089/cmb.2012.0021
22. Astashyn, A.; Tvedte, E.S.; Sweeney, D.; et al. Rapid and Sensitive Detection of Genome Contamination at Scale with FCS-GX. *Genome Biol* **2024**, *25*, 60. https://doi.org/10.1186/s13059-024-03198-7
23. Schloss, P.D.; Westcott, S.L.; Ryabin, T.; et al. Introducing Mothur: Open-Source, Platform-Independent, Community-Supported Software for Describing and Comparing Microbial Communities. *Appl Environ Microbiol* **2009**, *75*, 7537–7541. https://doi.org/10.1128/AEM.01541-09
24. Darling, A.C.; Mau, B.; Blattner, F.R.; Perna, N.T. Mauve: Multiple Alignment of Conserved Genomic Sequence with Rearrangements. *Genome Res* **2004**, *14*, 1394–1403. https://doi.org/10.1101/gr.2289704
25. Bortolaia, V.; Kaas, R.S.; Ruppe, E.; et al. ResFinder 4.0 for Predictions of Phenotypes from Genotypes. *J Antimicrob Chemother* **2020**, *75*, 3491–3500. https://doi.org/10.1093/jac/dkaa345
26. Maure, A.; Robino, E.; Van der Henst, C. The Intracellular Life of *Acinetobacter baumannii*. *Trends Microbiol* **2023**, *31*, 1238–1250. https://doi.org/10.1016/j.tim.2023.06.007
27. Manfi Ahmed, S.; Hashim Yaseen, K.; Mohammed Mahmood, M. Immunological Evaluation of Individuals Infected with *Acinetobacter baumannii*. *Arch Razi Inst* **2022**, *77*, 1813–1819. https://doi.org/10.22092/ARI.2022.357980.2126
28. Lescure, F.X.; Bouadma, L.; Nguyen, D.; et al. Clinical and Virological Data of the First Cases of COVID-19 in Europe: A Case Series. *Lancet Infect Dis* **2020**, *20*, 697–706. https://doi.org/10.1016/S1473-3099(20)30200-0
29. Ibrahim, S.; Al-Saryi, N.; Al-Kadmy, I.M.S.; Aziz, S.N. Multidrug-Resistant *Acinetobacter baumannii* as an Emerging Concern in Hospitals. *Mol Biol Rep* **2021**, *48*, 6987–6998. https://doi.org/10.1007/s11033-021-06690-6
30. Antimicrobial Resistance Collaborators. Global Burden of Bacterial Antimicrobial Resistance in 2019: A Systematic Analysis. *Lancet* **2022**, *399*, 629–655. https://doi.org/10.1016/S0140-6736(21)02724-0
31. Lau, M.Y.; Ponnampalavanar, S.; Chong, C.W.; et al. The Characterisation of Carbapenem-Resistant *Acinetobacter baumannii* and *Klebsiella pneumoniae* in a Teaching Hospital in Malaysia. *Antibiotics* **2024**, *13*, 1107. https://doi.org/10.3390/antibiotics13111107
32. Yu, K.; Zeng, W.; Xu, Y.; et al. Bloodstream Infections Caused by ST2 *Acinetobacter baumannii*: Risk F actors, Antibiotic Regimens, and Virulence over 6 Years Period in China. *Antimicrob Resist Infect Control* **2021**, *10*, 16. https://doi.org/10.1186/s13756-020-00876-6
33. Pustijanac, E.; Hrenović, J.; Vranić-Ladavac, M.; et al. Dissemination of Clinical Acinetobacter baumannii Isolate to Hospital Environment during the COVID-19 Pandemic. *Pathogens* **2023**, *12*, 410. https://doi.org/10.3390/pathogens12030410
34. Bedenić, B.; Bratić, V.; Mihaljević, S.; et al. Multidrug-Resistant Bacteria in a COVID-19 Hospital in Zagreb. *Pathogens* **2023**, *12*, 117. https://doi.org/10.3390/pathogens12010117
35. Zingg, S.; Kuster, S.; von Rotz, M.; et al. Outbreak with OXA-23-producing Acinetobacter baumannii in a COVID-19 ICU cohort: unraveling routes of transmission. *Antimicrob Resist Infect Control* **2024**, *13*, 127. https://doi.org/10.1186/s13756-024-01485-3
36. Cureño-Díaz, M.A.; Plascencia-Nieto, E.S.; Loyola-Cruz, M.Á.; et al. Gram-Negative ESKAPE Bacteria Surveillance in COVID-19 Pandemic Exposes High-Risk Sequence Types of *Acinetobacter baumannii* MDR in a Tertiary Care Hospital. *Pathogens* **2024**, *13*, 50. https://doi.org/10.3390/pathogens13010050